

*Invited Paper for the Annual Meeting of the Fluids Engineering Division of the
Korean Society of Mechanical Engineers, April, 1997.*

SOME CURRENT ADVANCES IN CAVITATION RESEARCH

Christopher E. Brennen
California Institute of Technology,
Pasadena, California 91125

Abstract

Several recent experimental and analytical investigations of cavitating flows have revealed new phenomena which clearly affect how we should view cavitation growth and collapse and the strategies used to ameliorate its adverse effects.

On the scale of individual bubbles it is now clear that the dynamics and acoustics of single bubbles are severely affected by the distortion of the bubble by the flow. This distortion depends on the typical dimension and velocity of the flow (as well as the Reynolds number) and therefore the distortion effects are very important in the process of scaling results up from the model to the prototype. The first part of the lecture will discuss the implications of these new observations for the classic problem of scale-up.

Another recent revelation is the importance of the interactions between bubbles in determining the coherent motions, dynamic and acoustic, of a cloud of cavitation bubbles. The second part of the lecture focusses on these cloud cavitation effects. It is shown that the collapse of a cloud of cavitating bubbles involves the formation of a bubbly shock wave and it is suggested that the focussing of these shock waves is responsible for the enhanced noise and damage in cloud cavitation. The paper describes experiments and calculations conducted to investigate these phenomena in greater detail as part of an attempt to find ways of ameliorating the most destructive effects associate with cloud cavitation.

1 Introduction

Historically, cavitation noise and damage have been visualized as resulting from the collapse of individual bubbles and the effects of the surrounding flow field and of neighboring bubbles have been largely ignored. It is now being recognized that both effects may have important consequences and that recognition of these effects leads to some new mitigation strategies. We begin in the next section with a review of single bubble dynamics in a typical flow field.

2 Dynamics of Single Bubbles

Recent research has shed new light on the effects of the flow on a single cavitation "event", the term used to denote the processes which follow when an individual cavitating nucleus is convected into a region of low pressure. The pioneering observations of single events which were made by Knapp (see, for example, Knapp and Hollander 1948) were followed by the analyses of Plesset (1949), Parkin (1952) and others who sought to model these observations of the growth and collapse of a travelling cavitation bubble using Rayleigh's equation for the dynamics of a spherical bubble (Rayleigh 1917). Some of the early (and classic) observations of individual travelling cavitation bubbles by Knapp and Hollander (1948), Parkin (1952) and Ellis (1952) make mention of the deformation of the bubbles by the flow. But the focus of attention soon shifted to the easier observations of the dynamics of individual bubbles in quiescent liquid and it is only recently that investigations of the deformation caused by the flow have resumed. Both Knapp and Hollander (1948) and Parkin (1952) observed that almost all cavitation bubbles are closer to hemispherical than spherical and that

they appear to be separated from the solid surface by a thin film of liquid. Such bubbles are clearly evident in other photographs of cavitation on a hydrofoil such as those of Blake *et al.* (1977) or Briançon-Marjollet *et al.* (1990).

It is important to consider the typical size of the cavitation bubbles relative to the thickness of the viscous boundary layer. In the flow of a uniform stream of velocity, U , around an object such as a hydrofoil with typical dimension, D , the thickness of the laminar boundary layer near the minimum pressure point will be given qualitatively by $\delta \approx (\nu D/U)^{\frac{1}{2}}$ where ν is the kinematic viscosity of the liquid. In contrast, the asymptotic growth rate of a bubble yields a typical maximum bubble radius, R_M , given by

$$R_M \approx 2D(-\sigma - C_{pmin}) \quad (1)$$

where σ is the cavitation number defined as $2(p_\infty - p_v)/\rho U^2$ where p_∞ and p_v are respectively the upstream and vapor pressures and ρ is the liquid density. The coefficient of pressure, C_p , is defined as $2(p - p_\infty)/\rho U^2$ where p is the local pressure in the flow and C_{pmin} denotes the minimum pressure coefficient in the flow. It follows that the ratio of the boundary layer thickness to the maximum bubble radius, δ/R_M , is given approximately by

$$\frac{\delta}{R_M} = \frac{1}{2(-\sigma - C_{pmin})} \left\{ \frac{\nu}{DU} \right\}^{\frac{1}{2}} \quad (2)$$

Therefore, provided $(-\sigma - C_{pmin})$ is of the order of 0.1 or greater, it follows that for the high Reynolds numbers, UD/ν , which are typical of most of the flows in which cavitation is a problem, the boundary layer is usually much thinner than the typical dimension of the bubble. This does not mean the boundary layer is unimportant. But we can anticipate that those parts of the cavitation bubble furthest from the solid surface will interact with the primarily inviscid flow outside the boundary layer, while those parts close to the solid surface will be affected by the boundary layer and the shear forces associated with it.

A number of recent research efforts have focussed on these bubble/flow interactions including the work of van der Meulen and van Renesse (1989) and Briançon-Marjollet *et al.* (1990). Recently, Ceccio and Brennen (1991) and Kuhn de Chizelle *et al.* (1994) have made an extended series of observations of cavitation bubbles in the flow around two axisymmetric headforms including studies of the scaling of the phenomena. For both headforms, the isobars in the neighbourhood of the minimum pressure point exhibit a large pressure gradient normal to the surface. This pressure gradient is associated with the curvature of the body in the vicinity of the minimum pressure point. Consequently, at a given cavitation number, σ , the region below the vapor pressure which is enclosed between the solid surface and the $C_p = -\sigma$ isobaric surface is long and thin compared with the size of the headform. Only nuclei which pass through this thin volume will cavitate.

Ceccio and Brennen (1991) made detailed observations of individual cavitation bubbles at relatively low Reynolds numbers. Typical photographs of the bubble during the cycle of bubble growth and collapse are shown in figure 1. The shape during the initial growth phase is that of a spherical cap, the bubble being separated from the headform surface by a thin layer of liquid of the same order of magnitude as the boundary layer thickness. Later developments depend on the geometry of the headform and the Reynolds number.

In the simplest cases and at relatively low Reynolds number the bubbles are as shown in figure 1. As the bubble begins to enter the region of adverse pressure gradient the exterior frontal surface is pushed inward causing the profile of the bubble to appear wedge-like. Thus the collapse is initiated on the exterior frontal surface of the bubble and this often leads to the bubble fission. But, two other processes are occurring at the same time. First, the streamwise thickness of the bubble decreases faster than its spanwise breadth (spanwise being defined as the direction parallel to the headform surface and normal to the oncoming stream) so that the largest dimension of the bubble is its spanwise breadth. Second, the bubble acquires significant spanwise vorticity through its interactions with the boundary layer during the growth phase. Consequently, as the collapse proceeds this vorticity is concentrated and the bubble evolves into one (or two or possibly more) cavitating vortices with spanwise axes. These vortex bubbles proceed to collapse and seem to rebound as a cloud of much smaller bubbles. Often a coherent second collapse of this cloud was observed when the bubbles were not too scattered by the flow. Ceccio and Brennen (1991) (see also Kumar and Brennen 1993b) conclude that the flow-induced fission prior to collapse can have a substantial effect on the noise impulse.

Two additional phenomena were observed on the headform which exhibited laminar boundary layer separation. The first of these was the observation that the layer of liquid underneath the bubble would become disrupted by some instability. As seen in figure 2 this results in a bubbly layer of fluid which

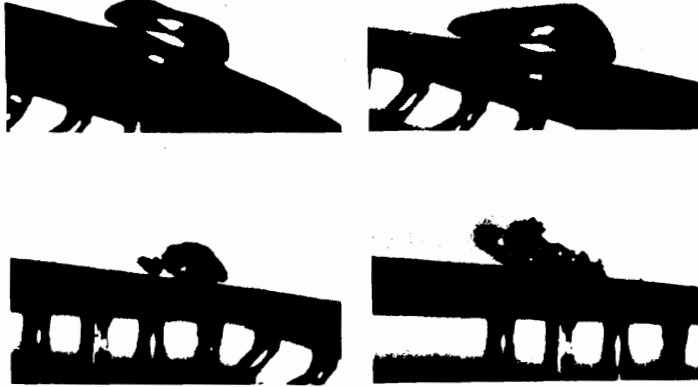


Figure 1: A series of photographs illustrating the growth and collapse of a travelling cavitation bubble in the flow around a 5.08cm diameter Schiebe headform at $\sigma = 0.45$ and a speed of 9 m/s. The order of development is top left, top right, bottom left, bottom right. The flow is from right to left. The scale is 4.5 times lifesize. From Ceccio and Brennen (1991).

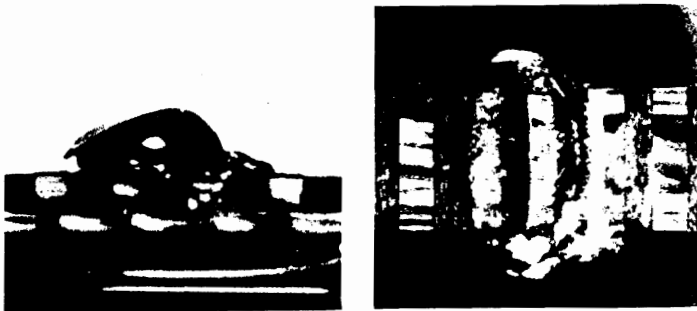


Figure 2: Simultaneous profile and plan views of illustrating the instability of the liquid layer under a travelling cavitation bubble (for $\sigma = 0.45$ and a speed of 8.7 m/s). From Ceccio and Brennen (1991), the photographs are 3.8 times lifesize.

subsequently gets left behind the main bubble. This instability of the liquid layer leads to another mechanism of bubble fission. Because it trails behind, the bubbly layer collapses after the main body of the bubble.

The second and perhaps more consequential phenomenon only occurs with the occasional bubble. Infrequently, when a bubble passes the point of laminar separation, it triggers the formation of local “attached cavitation” streaks at the lateral or spanwise extremities of the bubble as seen in figure 3. Then, as the main bubble proceeds downstream, these “streaks” or “tails” of attached cavitation are stretched out behind the main bubble, the trailing ends of the tails being attached to the solid surface. Subsequently, the main bubble collapses first leaving the “tails” to persist for a fraction longer as illustrated by the lower photograph in figure 3.

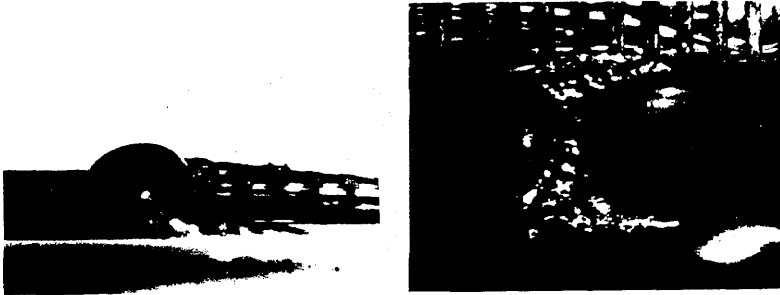


Figure 3: Simultaneous profile and plan views of a travelling cavitation bubble with attached tails (from Ceccio and Brennen 1991) at $\sigma = 0.42$ and a speed of 9 m/s . The photographs are 3.8 times lifesize.

We believe these tails occur when the trailing vortices fill with vapor/gas. The vortex lines emanating from the two sides of the bubble (as a result of its acquired circulation) must terminate on the solid surface of the body. For reasons which are unclear, these trailing vortices sometimes cavitate.

3 Scaling Effects for Single Bubbles

The importance of these occasional “events with tails” did not become clear until tests were conducted at much higher Reynolds numbers, with larger headforms (up to 50.5 cm in diameter) and somewhat higher speeds (up to 15 m/s). These tests were part of an investigation of the scaling of the bubble dynamic phenomena (Kuhn de Chizelle *et al.* 1994) which was conducted in the Large Cavitation Channel (LCC, Morgan 1990). One notable observation was the presence of a “dimple” on the exterior surface of all the individual travelling bubbles; examples of this dimple are included in figure 4. They are not the precursor to a re-entrant jet for the dimple seems to be relatively stable during most of the collapse process.

More importantly, it was observed that, at higher Reynolds number, “attached tails” occurred even on the headform which did not normally exhibit laminar separation. Moreover, the probability of occurrence of attached tails increased as the Reynolds number increased and the attached cavitation began to be more extensive. As the Reynolds number increased further, the bubbles would tend to trigger attached cavities over the entire wake of the bubble as seen in the lower two photographs in figure 4. Moreover the attached cavitation would tend to remain for a longer period after the main bubble had disappeared. Eventually, at the highest Reynolds numbers tested it appeared that the passage of a single bubble was sufficient to trigger a “patch” of attached cavitation (figure 4, bottom) which would persist for an extended period after the bubble had long disappeared.

This progression of events and the changes in the probabilities of the different kinds of events with Reynolds number imply a rich complexity in the micro-fluidmechanics of cavitation bubbles, much of which remains to be understood. Its importance lies in the fact that these different types of events cause differences in the collapse process which, in turn, alters the noise produced (see below) and, in all probability, the potential for cavitation damage.

When examined in retrospect, one can identify many of these phenomena in earlier photographic observations, including the pioneering, high-speed movies taken by Knapp. As previously remarked, Knapp and Hollander (1948), Parkin (1952) and others noted the spherical-cap shape of most travelling cavitation bubbles. More recently, Holl and Carroll (1979) observed a variety of different types of cavitation events on axisymmetric bodies and remarked that both travelling and attached cavitation “patches” occurred and could be distinguished from travelling bubble cavitation. A similar study of the different types of cavitation events was reported by Huang (1979) whose “spots” are synonymous with “patches”.

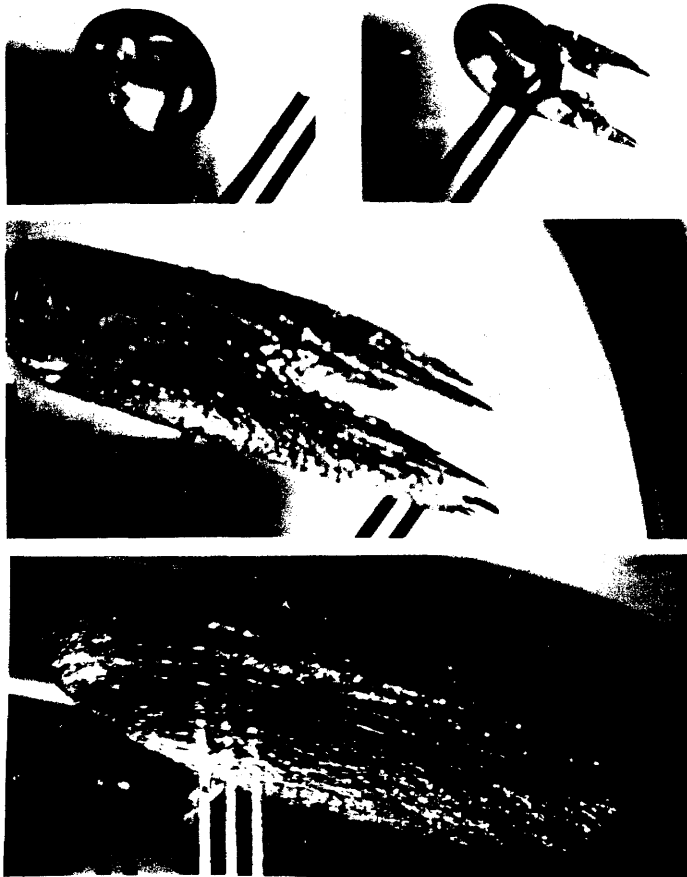


Figure 4: Typical cavitation events from the scaling experiments of Kuhn de Chizelle *et al.* (1994) showing an unattached bubble with “dimple” (upper left), a bubble with attached tails (upper right) and a transient bubble-induced patch (middle) all occurring on the 50.8cm diameter Schiebe headform at $\sigma = 0.605$ and a speed of 15 m/s. The bottom photograph shows a patch on the 25.4cm headform at $\sigma = 0.53$ and a speed of 15 m/s. The flow is from right to left. The top four are shown at 1.3 times lifesize and the bottom at 1.25 times lifesize.

4 Modelling the bubble dynamics

It is clear that the Rayleigh-Plesset analysis of a spherical bubble cannot reproduce many of the phenomena described in the preceding section. To study this further, Kuhn de Chizelle *et al.* (1994) developed an unsteady numerical code which models the bubbles using travelling sources and incorporates the distortion caused by the pressure gradients in the flow around the body. Only the irrotational flow outside of the boundary layer is addressed so the interaction of the bubble and the boundary layer is not treated by this method. The objective was to focus on the interaction of the bubble with the irrotational flow and the resulting shape of the exterior surface of the bubble. Different, viscous flow analyses would be needed to study the phenomena of the liquid layer instability and the triggering of attached cavitation.

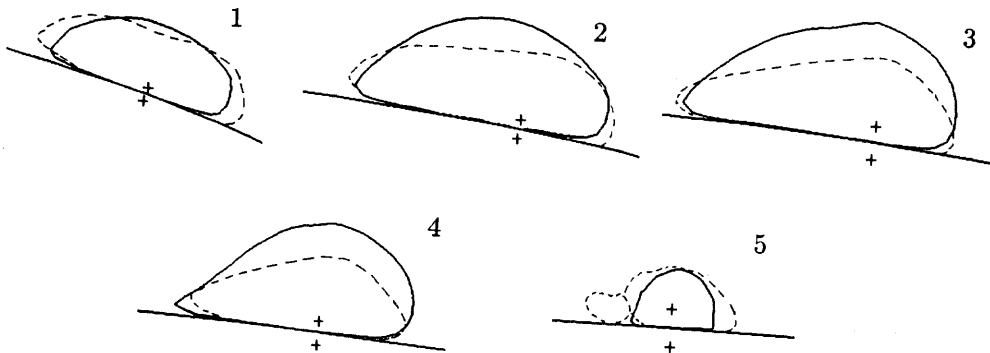


Figure 5: Comparison between the profiles of bubbles in figure 1 (dashed lines) and the profiles calculated by Kuhn de Chizelle *et al.* (1994) (solid lines) at five different moments during growth and collapse, consecutively numbered 1 through 5. The flow is from right to left. The locations of the source and the image source are shown by the crosses.

The basic, simplifying assumption behind the model is that the perturbations in the irrotational flow caused by the bubble can be fairly accurately modelled by a simple travelling source of adjustable intensity and position and that, once an image source is added to substantially satisfy the boundary condition on the headform surface, the remaining corrections which are required involve small modifications of the basic structure of the flow.

Typical results are presented in figure 5 where the bubble profiles from the photographs of figure 1 are compared with the profiles computed at the same five moments in time (labelled 1 to 5) during the bubble evolution. It can be seen that the overall size of the bubbles are in good agreement with the observations and that there is qualitative agreement in the general shape of the bubble as well as the way it changes with time. The program reproduces the spherical-cap shapes which are separated from the headform by a thin liquid layer. During the growth phase we note a minor depression in the top of the cap which is reminiscent of the dimples on the top of the bubbles observed by Kuhn de Chizelle *et al.* (1994) but is not as pronounced. Later the bubble assumes the wedge-like shape similar to the experiments. The computed bubbles are not, however, as elongated as those observed experimentally, particularly at the higher cavitation numbers; the probable reason for this is that the shape distortions which can be modelled by a single source are limited.

5 Single Bubble Noise

Improved understanding of the dynamics of individual cavitation events allows interpretation of the measurements of the noise produced by those events. In doing so we recognize that noise evaluation provides not only valuable practical information but is also useful as a diagnostic.

The radiated acoustic pressure, p_a , at a large distance, \mathcal{R} , from the center of a bubble of volume, $V(t)$, will be given by (Blake 1986, Brennen 1995)

$$p_a = \frac{\rho}{4\pi\mathcal{R}} \frac{d^2V}{dt^2} \quad (3)$$

It is clear that the noise pulse generated at bubble collapse results from the very large and positive values of d^2V/dt^2 which occur when the bubble is close to its minimum size. A good measure of the magnitude of the collapse pulse is the acoustic impulse, I , defined as the area under the pulse or

$$I = \int_{t_1}^{t_2} p_a dt \quad (4)$$

where t_1 and t_2 are times before and after the pulse at which p_a is zero. It is also useful in the present context to define a dimensionless impulse, I^* , as

$$I^* = 16\pi I\mathcal{R}/\rho U D^2 \quad (5)$$

where \mathcal{R} is now the distance from the cavitation event to the point of noise measurement and D is a typical dimension of the flow (such as the headform diameter). We shall compare the experimentally measured values of I^* from individual events on headforms of different size with those from numerical calculations of the growth and collapse of bubbles obtained from integration of the Rayleigh-Plesset equation. Details of these calculations are given in Ceccio and Brennen (1991) and Kuhn de Chizelle *et al.* (1994). For present purposes, we note that variations in the Weber number, Reynolds number and initial size of the nucleus had little effect on the computed impulses (within $\pm 10\%$).

For a range of experimental cavitation numbers, both Ceccio and Brennen (1991) and Kuhn de Chizelle *et al.* (1994) were able to identify within the hydrophone output the signal produced by each cavitation event and to measure the acoustic impulses of these events. The average values of the largest impulses obtained in this way are plotted against the maximum cavity volume in figure 6. In examining this particular correlation we follow the lead of Fitzpatrick and Strasberg (1956), Hamilton *et al.* (1982), Vogel *et al.* (1989) and others. Indeed, it was found that the correlation with maximum bubble volume was marginally better than the correlation with cavitation number (Kuhn de Chizelle *et al.* 1994). However, in viewing the data of figure 6 it must be emphasized that there is considerable variability in the magnitude of the impulses occurring at a particular operating condition. The standard deviations corresponding to the averaged I^* values of figure 6 are usually between 25% and 80% of the average value. But, in both sets of experiments an individual cavitation event (bubble) seems to be characterized by a fairly well-defined maximum possible value of the impulse. However the same conditions can also produce impulses which are a small fraction of this maximum.

Also shown in figure 6 is a hatched area which includes the results from the Rayleigh-Plesset calculations using the pressure distribution on the *surface* of the headform. Note first that the upper envelope of the experimental data for all the headforms and velocities is roughly consistent. However, this envelope of maximum values is approximately one order of magnitude smaller than the impulses obtained from the Rayleigh-Plesset calculations. There are probably two reasons for this. First, the actual maximum volume of the bubbles is significantly smaller than the maximum volume of the Rayleigh-Plesset bubbles as was documented by Kuhn de Chizelle *et al.* (1994). A second contributing factor to the discrepancy is that the more non-spherical the collapse, the less noise is produced since a spherical collapse produces the maximum focussing of the unsteady pressures. The interactions of the bubble with the pressure gradients and the boundary layer produce deformations in the shape which, in turn, alter the noise produced.

There is, however, another effect which is present in the data of figure 6. Virtually all of the data for a specific headform size and tunnel velocity tends first to increase as the maximum volume increases. However, in almost all cases, this trend reaches a maximum at a particular bubble volume and begins to decrease with further reduction in σ . This decrease is caused by a change in the dominant type of event as the bubble size increases. Kuhn de Chizelle *et al.* (1994) were able to demonstrate that events with tails are more likely to occur as the maximum bubble volume is increased and that such events produce much less noise, presumably because the tails cause further defocussing of the collapse.

In summary, we find that the micro-fluid-mechanics associated with individual events have an important effect on the noise produced by each event and that changes in the micro-fluid-mechanics with Reynolds number produce previously unrecognized scaling effects. However the overall trends are consistent with those predicted by the Rayleigh-Plesset or Fitzpatrick-Strasberg analysis though the maximum acoustic impulses are about an order of magnitude smaller than those of the spherical bubble analyses.

6 Cloud Cavitation

When the density of cavitation events increases in space or time and bubbles therefore begin to interact, a whole new set of phenomena may be manifest. The bubbles may begin to interact hydrodynamically with important consequences for both the global flow field, the global pressure field and therefore the dynamics and acoustics of the individual bubbles. In many flows of practical interest, "clouds" of cavitation bubbles

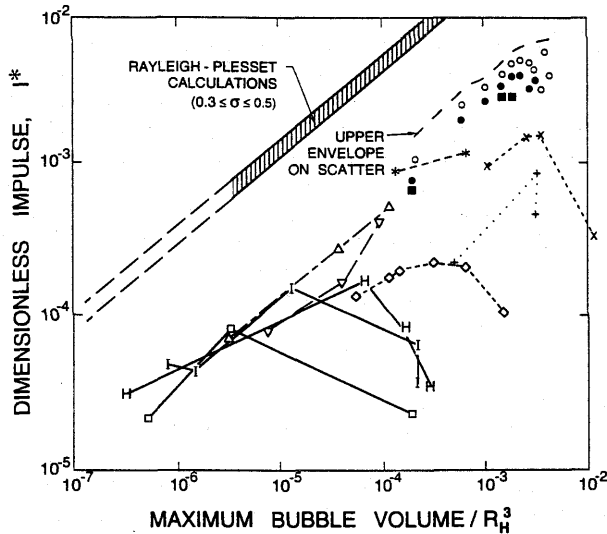


Figure 6: The dimensionless impulse, I^* , as a function of maximum volume of the bubble (divided by $D^3/8$). All the calculations using the Rayleigh-Plesset equation for $0.3 \leq \sigma \leq 0.5$ lie within the hatched region. The experimental measurements on a 5.08cm headform by Ceccio and Brennen (1991) are shown for $\sigma = 0.42$ (\odot), 0.45 (\bullet) and 0.50 (solid \square) along with the upper envelope which was defined by that data. The results of Kuhn de Chizelle *et al.* (1994) are shown for three headform diameters ($50.8\text{cm} =$ thick solid line, $25.4\text{cm} =$ thin solid line, $5.08\text{cm} =$ dotted line) at three different tunnel velocities ($9\text{m/s} = +, \Delta, \square$, $11.5\text{m/s} = \times, \nabla, \text{H}$, $15\text{m/s} = *, \diamond, \text{I}$).

are periodically formed and then collapse. This temporal periodicity may occur naturally as a result of the shedding of bubble-filled vortices or it may be the response to a periodic disturbance imposed on the flow. Common examples of imposed fluctuations are the interaction between rotor and stator blades in a pump or turbine and the interaction between a ship's propeller and the non-uniform wake created by the hull. In many of these cases the coherent collapse of the cloud of bubbles can cause more intense noise and more potential for damage than in a similar non-fluctuating flow.

Much recent interest has focused on the dynamics and acoustics of finite clouds of cavitation bubbles because of these very destructive effects (see, for example, Knapp (1955), Bark and van Berlekom 1978, Soyama *et al.* 1992). Here we address the issue of the modelling of the dynamics of cavitation clouds, a subject whose origins can be traced to the work of van Wijngaarden (1964) who first attempted to model the behavior of a collapsing layer of bubbly fluid next to a solid wall. In recent times, the literature on the linearized dynamics of clouds of bubbles has grown rapidly (see, for example, Orta 1987, d'Agostino *et al.* 1983, 1988, 1989, Prosperetti 1988). However, apart from some weakly non-linear analyses (Kumar and Brennen 1991, 1992, 1993b) only a few papers have addressed the highly non-linear processes involved during the collapse of a cloud of bubbles.

Another perspective on the subject of collapsing clouds was that introduced by Mørch and Kedrinskii and their co-workers (Mørch 1980, 1981, 1982, Hanson *et al.* 1981). They surmised that the collapse of a cloud of bubbles involves the formation and inward propagation of a shock wave and that the geometric focusing of this shock at the center of cloud creates the enhancement of the noise and damage potential associated with cloud collapse.

7 Dynamics of a Spherical Cloud

Most recently Wang and Brennen (1994, 1995, 1997) and Brennen *et al.* (1995) have used the mixture models employed earlier by d'Agostino *et al.* (1983, 1988, 1989) to study the non-linear growth and collapse of a spherical cloud of bubbles. A finite cloud of nuclei is subjected to an episode of low pressure which causes the cloud to cavitate; the pressure then returns to the original level causing the cloud to collapse. The initial pressure level is characterized by a cavitation number, σ , and the low pressure episode is characterized by a minimum pressure coefficient, C_{pmin} , and a duration, D/U , where D and U are respectively the typical dimension and velocity of the cavitating flow. The initial radius and void fraction of the cloud are denoted by A_0 and α_0 respectively and the initial radius of the bubbles within the cloud is denoted by R_0 .

In carrying out numerical calculations of this characteristic cloud cavitation problem, Wang and Brennen (1994, 1995, 1997) found that the "cloud interaction" parameter, β , defined as

$$\beta = \alpha_0(1 - \alpha_0)A_0^2/R_0^2 \quad (6)$$

is crucially important for the dynamics and acoustics of the cloud. Earlier linear and weakly nonlinear studies of cloud dynamics (d'Agostino & Brennen 1983, 1989; Kumar & Brennen 1991, 1992, 1993) showed that the cloud natural frequency is strongly dependent on this parameter. If β is small, the natural frequency of the cloud is close to that of the individual bubbles in the cloud. In other words, the bubbles in the cloud tend to behave as individual units in an infinite fluid and the bubble/bubble interaction effects are minor. On the other hand bubble interaction effects dominate when the value of β is greater than order one. Then the collective oscillation of bubbles in the cloud results in a cloud natural frequency which is lower than the natural frequency of individual bubbles.

Some of the results obtained by Wang and Brennen are shown in figures 7, 8 and 9. Figures 7 and 9 present examples of the bubble-size time history for five different Lagrangian radial locations, r_0 , within the cloud, from the surface, $r_0 = A_0$, to the centre, $r_0 = 0$. Figure 7 is for a large value of β in which the bubble interaction effects are strong. All the bubbles in the cloud grow almost in phase. However, because of the strong bubble/bubble interaction, bubble growth is severely constrained and the bubble growth rate within the cloud is much smaller than that near the surface. In other words, the bubbles in the interior are shielded by the outer shell of bubbles and grow to a smaller maximum size. This shielding effect is typical of the bubble/bubble interaction phenomenon in cavitating cloud dynamics (d'Agostino & Brennen 1983, 1989; Omta 1987; Smereka & Banerjee 1988; Chahine & Duraiswami 1992).

In the case of large β , as illustrated in figure 7, the bubbles on the surface of the cloud collapse first and the collapse propagates inward creating a bubbly shock wave. Figure 8 shows the spatial distribution of bubble radius and pressure at one moment in time when the shock wave has progressed inward to a position about half the Lagrangian radius of the cloud. The structure of this shock is very similar to those in the bubbly flows investigated by Noordij and van Wijngaarden (1974) and other investigators (see, for example, Brennen 1995, Kameda and Matsumoto 1995); the shock is comprised of a series of rebounds and secondary collapses which probably produce a ringing in the radiated sound. The locations with small bubble size represent regions of low void fraction and higher pressure due to the local bubble collapse.

As the shock front passes bubbles and causes them to collapse, a very large pressure pulse is produced, as shown in figure 8. The shock wave strengthens considerably as it propagates into the cloud primarily because of geometric focusing. One consequence of this can be seen in figure 7; the closer the bubbles are to the cloud centre, the smaller the size to which they collapse. Very complicated bubble-bubble interactions are observed and very high pressures are generated when the focusing shock reaches the centre of the cloud. Then a spreading expansion wave causes all bubbles to grow and begins another cycle of cloud oscillation.

Very different dynamics are manifest when the cloud interaction parameter is small and a typical bubble time history under these conditions is shown in figure 9 which should be contrasted with figure 7. Now, the bubbles grow more "freely" to a large size. However, the bubbles close to cloud centre still grow more slowly than the bubbles near the surface and, consequently, the maximum size of the bubbles on the surface can be up to an order of magnitude larger. As a result, the central bubbles collapse first and the collapse spreads outward as an expansion wave. There is no shock-enhancing process involved and the resulting noise produced is much smaller.

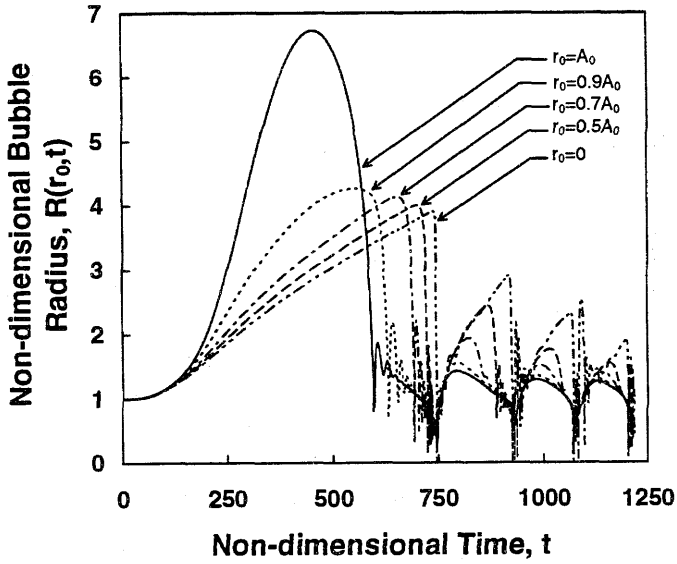


Figure 7: The time history of the dimensionless bubble size at five different positions in the cloud for $\sigma = 0.45$, $C_{pmin} = -0.75$, $\alpha_0 = 3\%$, $A_0 = 100$, and $D/A_0 = 5$. The cloud interaction parameter, β , is approximately 300 in this case.

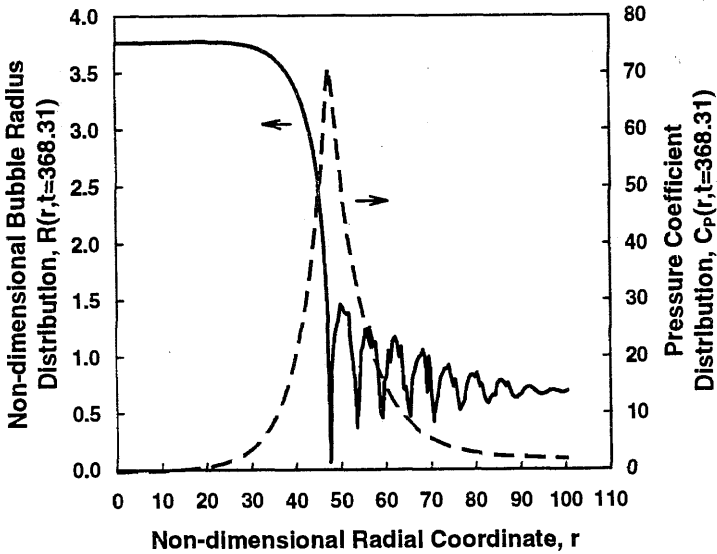


Figure 8: Bubble size and pressure distributions in the shock wave at a sample moment in time, $t = 368.31$. Parameters are $\sigma = 0.45$, $C_{pmin} = -0.75$, $\alpha_0 = 0.5\%$, $A_0 = 100$, and $D/A_0 = 2.5$.

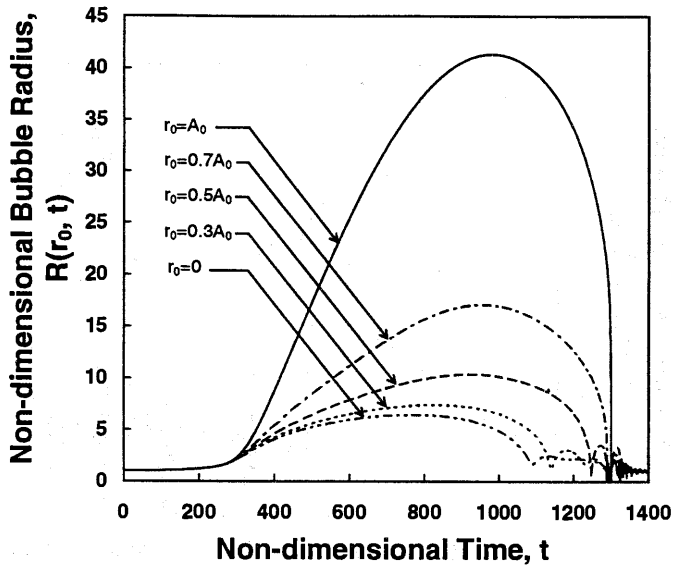


Figure 9: The time history of the dimensionless bubble size at five different positions in the cloud for $\alpha_0 = 0.03\%$ and $D/A_0 = 10$. Other parameters as in figure 7. The cloud interaction parameter, $\beta \approx 3$.

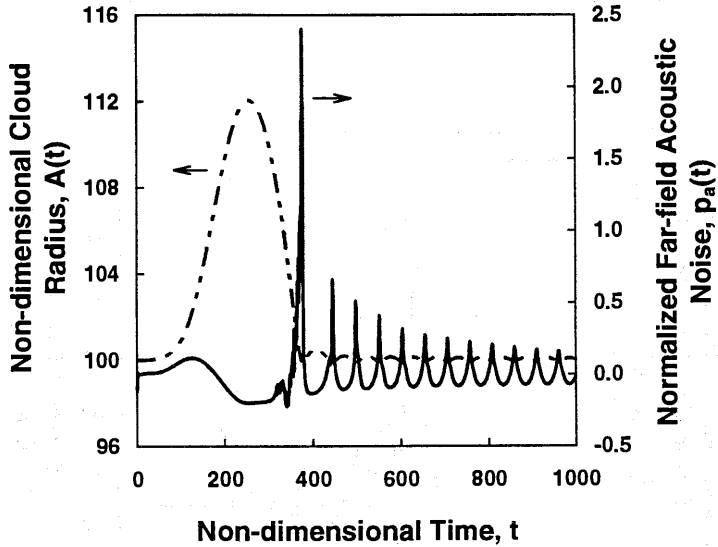


Figure 10: The time history of the dimensionless cloud radius and the resulting far-field acoustic noise for the case of figure 8.

8 Radiated Noise

It is important to determine the acoustic consequences associated with the cloud dynamics described above. For this reason we examine the far-field acoustic noise produced by the volumetric acceleration of the cloud. If we denote the dimensional time-varying volume of the cloud by $V(t)$, it follows that the dimensional form

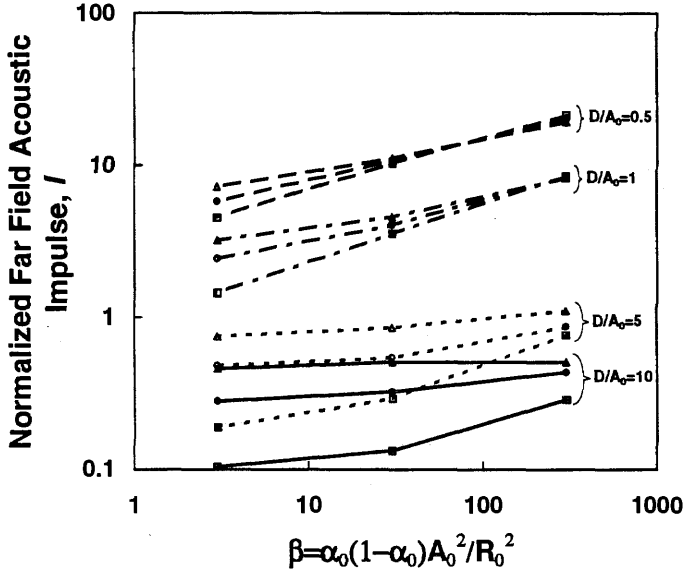


Figure 11: The impulse of the normalized far-field acoustic noise, I , as a function of the cloud interaction parameter, β , for different values of D/A_0 and three cavitation numbers, σ ($0.45 = \Delta$, $0.55 = \circ$, $0.65 = \square$). Other parameters are $C_{pmin} = -0.75$ and $A_0/R_0 = 100$.

of the time-varying far-field acoustic pressure is given by (Blake 1986)

$$p_a(t) = \frac{\rho_L}{4\pi\mathcal{R}} \frac{d^2V(t)}{dt^2} \quad (7)$$

where p_a is the radiated acoustic pressure and \mathcal{R} is the distance from the cloud centre to the point of measurement. The acoustic effects generated by individual bubbles are minor in the far-field and will be neglected. Then the radiated noise is simply given by the volume of the cloud and a typical calculation of the cloud radius and the far-field noise is presented in figure 10 for a case in which $\beta \gg 1$. Note that, unlike a single bubble, the cloud only decreases to a size marginally smaller than its equilibrium size during the collapse process. However, the local void fraction within the cloud undergoes large changes. (This is consistent with the recent experimental observations of cloud collapse by Reisman and Brennen (1996).) When the enhanced shock wave reaches the center of the cloud, extremely high radiated noise is produced. Subsequent cloud collapses also produced radiated pulses. Normally, after several collapse and rebound cycles, the cloud will begin to oscillate at its natural frequency.

The far-field acoustic impulse, I , is defined as the area under the largest pulse of the pressure signal or

$$I = \int_{t_1}^{t_2} p_a(t) dt, \quad (8)$$

where t_1 and t_2 are times before and after the pulse at which the acoustic pressure, p_a , is zero. Figure 11 presents the acoustic impulse as a function of the cloud interaction parameter, β , for flows with different cavitation numbers, σ , and different ratios of D/A_0 . In all cases, the impulse increases with increasing β , demonstrating quite explicitly the magnification in the cavitation noise produced by the coherent interacting dynamics of bubbles in a cloud.

9 Observations of Cloud Cavitation

Of course, in many flows of practical interest cloud cavitation has a much more complex geometry. Numerous investigators (Knapp 1955, Wade and Acosta 1966, Bark and van Berlekom 1978, Shen and Peterson 1978, 1980, Blake *et al.* 1977, Bark 1985, Lush and Skipp 1986, Franc and Michel 1988, Hart *et al.* 1990, Kubota *et al.* 1989, 1992, Le *et al.* 1993, de Lange *et al.* 1994, Kawanami *et al.* 1996) have studied the complicated flow patterns involved in the production and collapse of cloud cavitation on a hydrofoil. The basic features of the cyclic process of cloud formation and collapse (whether on a stationary or oscillating foil) are as follows. The growth phase usually involves the expansion of a single attached cavity, at the end of which a re-entrant jet penetrates the cavity from the closure region. This penetration breaks the cavity into a bubbly cloud which collapses as it is convected downstream.

The radiated noise all occurs during this bubbly part of the cycle. It consists of pressure pulses of very short duration and large magnitude; they are qualitatively similar to those calculated for the spherical cloud. The pulses have been measured Bark (1985), Bark and van Berlekom (1978), Le *et al.* (1993), Shen and Peterson (1978, 1980), McKenney and Brennen (1994), Reisman *et al.* (1994). More recently, Reisman and Brennen (1997) have made measurements of the impulsive pressures on the suction surface of a hydrofoil (within the cloud cavitation) simultaneous with radiated pulse measurements and high-speed movies. Very large pressure pulses were recorded by the surface transducers, with typical magnitudes as large as 10bar and durations of the order of 10^{-4} s. These are certainly sufficient to explain the enhanced noise and cavitation damage associated with cloud cavitation. For example, the large impulsive surface loadings due to these pulses could be responsible for the foil damage reported by Morgan (1995), who observed propeller blade trailing edges bent away from the suction surface and toward the pressure surface.

Reisman and Brennen (1997) also correlated the movies with the pressure measurements and found that the pressure pulses recorded (both on the foil surface and in the far field) are clearly associated with specific structures (more precisely, the dynamics of specific structures) which are visible in the movies. Indeed, it appears that several types of propagating structures (shock waves) are formed in a collapsing cloud and dictate the dynamics and acoustics of collapse. One type of shock wave structure is associated with the coherent collapse of a well-defined and separate bubble cloud when it is convected into a region of low pressure. This type of structure causes the largest impulsive pressures and radiated noise. The pulses it produces are termed *global* pulses since they are recorded almost simultaneously by all transducers. Figure 12 depicts four consecutive frames from one such movie; the cavitation cloud which is the remnant of the attached sheet cavity undergoes a rapid and coherent collapse between frames (b) and (c) of this figure. The collapse of this region radiates a pressure pulse which is detected by all the transducers. Note from figure 12, that global cloud collapses do not involve large changes in the overall dimensions of the cloud, a feature which is consistent with the calculations of the last section (see figure 10). Rather collapse involves large changes in the void fraction distribution within the cloud. The global collapse often generates multiple pulses which may represent several shock focussing events.

But, unexpectedly, two other types of structures were observed. Typically, their pulses are recorded by only one transducer and these events are therefore called *local* pulses. They are observed to occur when a shock structure passes over the face of the transducer. While these *local* events are smaller and therefore produce less radiated noise, the pressure pulse magnitudes are almost as large as those produced by *global* events. The two types of structures which are observed to cause local pulses are termed "crescent-shaped regions" and "leading edge structures"; both occur during the less coherent collapse of clouds.

The first type of flow structure (illustrated in photographs (a) through (c) of figure 13) is a crescent-shaped region of low void fraction. These crescent-shaped regions appear randomly in the bubbly mixture which remains after the passage of the reentrant jet. A close look at photograph (c) shows how complicated these flow structures can be since this crescent-shaped region appears to have some internal structure. Photographs (b) and (c) also show that more than one crescent-shaped structure can be present at any moment in time.

In addition, the movie and pressure data consistently displayed a local pulse when the upstream boundary, or leading edge, of the detached bubbly mixture passed over a transducer. This second type of local flow structure which also produces a local pulse is illustrated in photograph (d) of figure 13. These "leading edge structures" are created when the sheet cavity detaches from the foil and they propagate downstream faster than the mixture velocity.

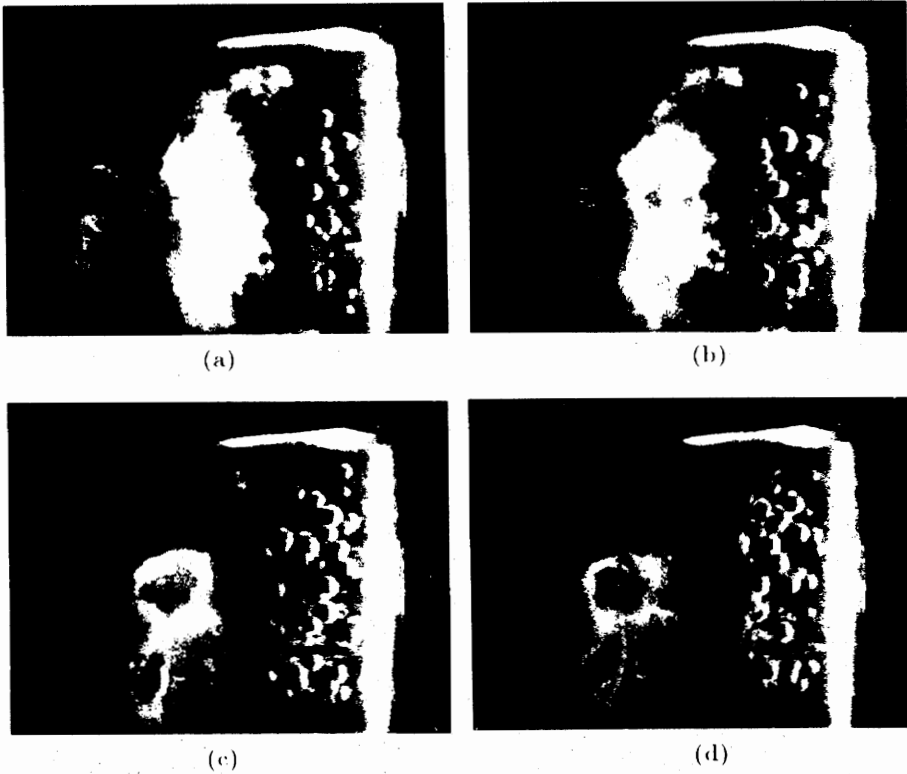


Figure 12: Consecutive high speed movie frames ($2ms$ apart) of cavitation on the suction surface of cavitating foil. The flow is from right to left. A global cloud collapse occurs between frames (b) and (c). From Reisman and Brennen (1997).

Parenthetically, we note that injection of air into the cavitation on the suction surface can substantially reduce the magnitude of the pressure pulses produced (Ukon 1986, Arndt *et al.* 1993, Reisman *et al.* 1997). However Reisman *et al.* (1997) have shown that the bubbly shock wave structures still occur; but with the additional air content in the bubbles, the pressure pulse is greatly reduced.

10 Concluding Comments

In this paper we have summarized some of the recent advances in our understanding of travelling bubble cavitation and cloud cavitation. We have demonstrated that individual cavitating bubbles or events display a rich variety of fluid mechanical phenomena as the bubbles interact with the largely irrotational flow outside the boundary layer and with the boundary layer itself. Many of the observed phenomena remain to be understood, particularly the instability of the thin liquid layer underneath the bubble and the separation phenomena induced by the passage of the bubble. It has been demonstrated that these micro-fluid-mechanical effects are important because they influence the coherence of the collapse and therefore the noise and damage potential produced by individual bubbles. It seems possible that surface modifications (for example, surface roughening) could significantly alter these micro-fluid-mechanical processes and therefore alter the noise and damage potential. This suggests a number of options which remain to be explored.

It is also becoming clear that effects of the interaction between bubbles may be crucially important especially when they give rise to the phenomena called cloud cavitation. Calculations of the growth and

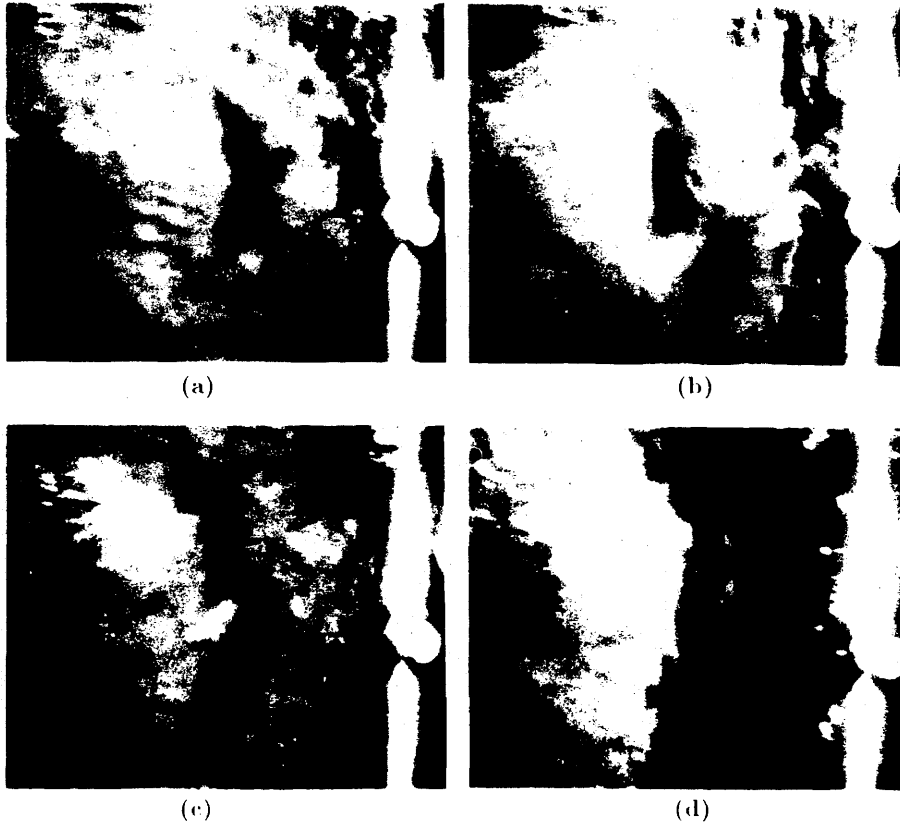


Figure 13: Local pulse structures in the cavitation on the suction surface of a cavitating foil. The flow is from right to left. Crescent-shaped structures are seen in (a), (b), and (c) and a leading edge event with two collapses is shown in photograph (d). From Reisman and Brennen (1997).

collapse of a spherical cloud of cavitating bubbles confirm the earlier work of Mørch, Kedrinskii and their co-workers, namely that, provided the cloud interaction parameter (β) is large enough, collapse occurs first on the surface of the cloud. The inward propagating collapse front becomes a bubbly shock wave which grows in magnitude due to geometric focussing. Very large pressures and radiated impulses occur when the shock reaches the center of the cloud.

Of course, actual clouds are far from spherical. And, even in a homogeneous medium, gasdynamic shock focussing can be quite complex and involve significant non-linear effects (see, for example, Sturtevant and Kulkarny 1976). Nevertheless, it seems evident that once collapse is initiated on the surface of a cloud, the propagating shock will focus and produce large local pressure pulses and radiated acoustic pulses. It is not, however, clear exactly what form the foci might take in the highly non-uniform, three-dimensional bubbly environment of a cavitation cloud on a hydrofoil, for example.

The experiments with hydrofoils experiencing cloud cavitation have shown that very large pressure pulses occur within the cloud and are radiated away from it during the collapse process. Within the cloud, these pulses can have magnitudes as large as 10bar and durations of the order of $10^{-4}s$. These are certainly sufficient to explain the enhanced noise and cavitation damage associated with cloud cavitation. Moreover, these pressure pulses are associated with several distinct shock structures which can be observed visually and which propagate through the bubbly mixture.

Thus we suggest a new perspective on cavitation damage and noise in flows which involve large collections

of cavitation bubbles with a sufficiently large void fraction (or, more specifically, a large enough β) so that the bubbles interact and collapse coherently. This view maintains that the cavitation noise and damage is generated by the formation and propagation of bubbly shock waves within the collapsing cloud. The experiments reveal several specific shock wave structures. One of these is the mechanism by which the large coherent collapse of a finite cloud of bubbles occurs. A more unexpected result was the discovery of more localized bubbly shock waves propagating within the bubbly mixture in several forms, as crescent-shaped regions and as leading edge structures. These seem to occur when the behavior of the cloud is less coherent. They produce surface loadings which are within an order of magnitude of the more coherent events and could also be responsible for cavitation damage. However, because they are more localized, the radiated noise they produce is much smaller than that due to global events.

The phenomena described are expected to be important features in a wide range of cavitating flows. However, the analytical results clearly suggest that the phenomena may depend strongly on the cloud interaction parameter, β . If this is the case, some very important scaling effects may occur. It is relatively easy to envision a situation in which the β value for some small scale model experiments is too small for cloud effects to be important but in which the prototype would be operating at a much larger β due to the larger cloud size, A_0 (assuming the void fractions and bubble sizes are comparable). Under these circumstances, the model would not manifest the large cloud cavitation effects which could occur in the prototype.

In conclusion, these recent investigations provide new insights into the dynamics and acoustics both of individual cavitation bubbles and of clouds of bubbles. In turn, these insights suggest new ways of modifying and possibly ameliorating cavitation noise and damage.

11 Acknowledgements

My profound thanks to the graduate students who contributed to the results described, Luca d'Agostino, Steven Ceccio, Douglas Hart, Sanjay Kumar, Yan Kuhn de Chizelle, Beth McKenney, Zhenhuan Liu, Yi-Chun Wang and Garrett Reisman. As always, Allan Acosta provided valuable insights and inspiration. I am also deeply grateful for the support of the Office of Naval Research who sponsored much of the research and supported the preparation of this paper under Contracts N00014-91-J-1295 and N00014-97-1-0002.

12 References

- Arndt, R.E.A., Ellis, C.R. and Paul, S., "Preliminary investigation of the use of air injection to mitigate cavitation erosion," *Proc. ASME Symp. on Bubble Noise and Cavitation Erosion in Fluid Systems*, 1993, FED-Vol.176, pp. 105-116.
- Bark, G. and van Berlekom, W.B., "Experimental investigations of cavitation noise," *Proc. 12th ONR Symp. on Naval Hydrodynamics*, 1978, pp. 470-493.
- Bark, G., "Developments of distortions in sheet cavitation on hydrofoils," *Proc. ASME Int. Symp. on Jets and Cavities*, 1985, pp. 215-225.
- Blake, W. K., Wolpert, M. J. and Geib, F. E., "Cavitation noise and inception as influenced by boundary-layer development on a hydrofoil," *J. Fluid Mech.*, 1977, Vol. 80, pp. 617-640.
- Blake, W.K., "Mechanics of flow-induced sound and vibration," Academic Press, 1986.
- Brennen, C.E., "Cavitation and bubble dynamics," Oxford University Press, 1995.
- Brennen, C.E., Reisman, G.E. and Wang, Y.-C., "Shock waves in cloud cavitation," *Proc. 21st ONR Symp. on Naval Hydrodynamics*, 1996.
- Briançon-Marjolle, L., Franc, J.P. and Michel, J.M., "Transient bubbles interacting with an attached cavity and the boundary layer," *J. Fluid Mech.*, 1990, Vol. 218, pp. 355-376.
- Ceccio, S.L. and Brennen, C.E., "Observations of the dynamics and acoustics of travelling bubble cavitation," *J. Fluid Mech.*, 1991, Vol. 233, pp. 633-660.

- Chahine, G.L. and Duraiswami, R., "Dynamical interactions in a multibubble cloud," *ASME J. Fluids Eng.*, 1992, Vol. 114, pp. 680-686.
- d'Agostino, L. and Brennen, C.E., "On the acoustical dynamics of bubble clouds," *ASME Cavitation and Multiphase Flow Forum*, 1983, pp. 72-75.
- d'Agostino, L. and Brennen, C.E., "Acoustical absorption and scattering cross-sections of spherical bubble clouds," *J. Acoust. Soc. of Amer.*, 1988, Vol. 84, No.6, pp. 2126-2134.
- d'Agostino, L. and Brennen, C.E., "Linearized dynamics of spherical bubble clouds," *J. Fluid Mech.*, 1989, Vol. 199, pp. 155-176.
- de Lange, D.F., de Bruin, G.J. and van Wijngaarden, L., "On the mechanism of cloud cavitation - experiment and modeling," *Proc. 2nd Int. Symp. on Cavitation, Tokyo*, 1994, pp. 45-50.
- Ellis, A.T., "Observations on cavitation bubble collapse," *Calif. Inst. of Tech. Hydr. Lab. Rep.*, 1952, No. 21-12.
- Fitzpatrick, H.M. and Strasberg, M., "Hydrodynamic sources of sound," *Proc. First ONR Symp. on Naval Hydrodynamics*, 1956, pp. 241-280.
- Franc, J.P. and Michel, J.M., "Unsteady attached cavitation on an oscillating hydrofoil," *J. Fluid Mech.*, 1988, Vol. 193, pp. 171-189.
- Hamilton, M.F., Thompson, D.E. and Billet, M.L., "An experimental study of traveling bubble cavitation and noise," *Proc. ASME Int. Symp. on Cavitation Noise*, 1982, pp. 25-33.
- Hanson, I., Kedrinskii, V.K. and Mørch, K.A., "On the dynamics of cavity clusters," *J. Appl. Phys.*, 1981, Vol. 15, pp. 1725-1734.
- Hart, D.P., Brennen, C.E. and Acosta, A.J., "Observations of cavitation on a three dimensional oscillating hydrofoil," *ASME Cavitation and Multiphase Flow Forum*, 1990, FED-Vol. 98, pp. 49-52.
- Holl, J.W. and Carroll, J.A., "Observations of the various types of limited cavitation on axisymmetric bodies," *Proc. ASME Int. Symp. on Cavitation Inception*, 1979, pp. 87-99.
- Huang, T.T., "Cavitation inception observations on six axisymmetric headforms," *Proc. ASME Int. Symp. on Cavitation Inception*, 1979, pp. 51-61.
- Kameda, M. and Matsumoto, Y., "Structure of shock waves in a liquid containing gas bubbles," *IUTAM Symp. on Waves in Liquid/Gas and Liquid/Vapour Two-Phase Systems*, 1995, pp. 117-126.
- Kawanami, Y., Kato, H., Yamaguchi, H., Tagaya, Y. and Tanimura, M., "Mechanism and control of cloud cavitation," *Proc. ASME Symp. on Cavitation and Gas-Liquid Flows in Fluid Machinery and Devices*, 1996, FED-Vol. 236, pp. 329-336.
- Knapp, R.T., "Recent investigations of the mechanics of cavitation and cavitation damage," *Trans. ASME*, 1955, Vol. 77, pp. 1045-1054.
- Knapp, R.T. and Hollander, A., "Laboratory investigations of the mechanisms of cavitation," *Trans. ASME*, 1948, Vol. 70, p. 419.
- Kubota, A., Kato, H., Yamaguchi, H. and Maeda, M., "Unsteady structure measurement of cloud cavitation on a foil section using conditional sampling," *ASME J. Fluids Eng.*, 1989, Vol. 111, pp. 204-210.
- Kubota, A., Kato, H. and Yamaguchi, H., "A new modelling of cavitating flows - a numerical study of unsteady cavitation on a hydrofoil section" *J. Fluid Mech.*, 1992, Vol. 240, pp. 59-96.
- Kuhn de Chizelle, Y., Ceccio, S.L. and Brennen, C.E., "Observations, scaling and modelling of travelling bubble cavitation", *J. Fluid Mech.*, 1994, Vol. 293, pp. 99-126.

- Kumar, S. and Brennen, C.E., "Non-linear effects in the dynamics of clouds of bubbles," *J. Acoust. Soc. Am.*, 1991, Vol. 89, pp. 707-714.
- Kumar, S. and Brennen, C.E., "Harmonic cascading in bubble clouds," *Proc. Int. Symp. on Propulsors and Cavitation, Hamburg*, 1992, pp. 171-179.
- Kumar, S. and Brennen, C.E., "A study of pressure pulses generated by travelling bubble cavitation," *J. Fluid Mech.*, 1993a, Vol. 255, pp. 541-564.
- Kumar, S. and Brennen, C.E., "Some nonlinear interactive effects in bubbly cavitating clouds," *J. Fluid Mech.*, 1993b, Vol. 253, pp. 565-591.
- Le, Q., Franc, J. M. and Michel, J. M., "Partial cavities: global behaviour and mean pressure distribution", *ASME J.Fluids Eng.*, 1993, Vol. 115, pp. 243-248.
- Lush, P.A. and Skipp, S.R., "High speed cine observations of cavitating flow in a duct," *Int. J. Heat and Fluid Flow*, 1986, Vol. 7, pp. 283-290.
- McKenney, E.A. and Brennen, C.E., "On the dynamics and acoustics of cloud cavitation on an oscillating hydrofoil," *Proc. ASME Symp. on Cavitation and Gas-Liquid Flows in Fluid Machinery and Devices*, 1994, FED-Vol.190, pp. 195-202.
- Mørch, K.A., "On the collapse of cavity cluster in flow cavitation," *Proc. First Int. Conf. on Cavitation and Inhomogenities in Underwater Acoustics, Springer Series in Electrophysics*, 1980, Vol. 4, pp. 95-100.
- Mørch, K.A., "Cavity cluster dynamics and cavitation erosion," *Proc. ASME Cavitation and Polyphase Flow Forum*, 1981, pp. 1-10.
- Mørch, K.A., "Energy considerations on the collapse of cavity cluster," *Appl. Sci. Res.*, 1982, Vol. 38, p. 313.
- Morgan, W.B., "David Taylor Research Center's Large Cavitation Channel," *Proc. Int. Towing Tank Conference, Madrid, Spain.*, 1990.
- Morgan, W.B., personal communication, 1995.
- Noordij, L. and van Wijngaarden, L., "Relaxation effects, caused by relative motion, on shock waves in gas-bubble/liquid mixtures," *J. Fluid Mech.*, 1974, Vol. 66, pp. 115-143.
- Omta, R., "Oscillations of a cloud of bubbles of small and not so small amplitude," *J. Acoust. Soc. Am.*, 1987, Vol. 82, pp. 1018-1033.
- Parkin, B.R., "Scale effects in cavitating flow," *Ph.D. Thesis, Calif. Inst. of Tech.*, 1952.
- Plesset, M.S., "The dynamics of cavitation bubbles," *ASME J. Appl. Mech.*, 1949, Vol. 16, pp. 228-231.
- Prosperetti, A., "Bubble-related ambient noise in the ocean," *J. Acoust. Soc. Am.*, 1988, Vol. 84, pp. 1042-1054.
- Reisman, G.E., McKenney, E.A. and Brennen, C.E., "Cloud cavitation on an oscillating hydrofoil", *Proc. 20th ONR Symp. on Naval Hydrodynamics*, 1994, pp. 78-89.
- Reisman, G.E. and Brennen, C.E., "Experimental observations of shock waves in cloud cavitation," 1997, submitted to *J. Fluid Mech.*.
- Reisman, G.E., "Dynamics, acoustics and control of cloud cavitation on hydrofoils," 1997, Ph.D. thesis, Cal. Inst. of Tech.
- Reisman, G.E., Duttweiler, M.E. and Brennen, C.E., "Effect of air injection on the cloud cavitation of a hydrofoil," *ASME Fluids Engineering Conference*, 1997.

- Shen, Y. and Peterson, F.B., "Unsteady cavitation on an oscillating hydrofoil," *Proc. 12th ONR Symp. on Naval Hydrodynamics*, 1978, pp. 362-384.
- Shen, Y. and Peterson, F.B., "The influence of hydrofoil oscillation on boundary layer transition and cavitation noise," *Proc. 13th ONR Symp. on Naval Hydrodynamics*, 1980, pp. 221-241.
- Smereka, P. and Banerjee, S., "The dynamics of periodically driven bubble clouds," *Phys. Fluids*, 1988, Vol. 31, pp. 3519-3531.
- Soyama, H., Kato, H. and Oba, R., "Cavitation observations of severely erosive vortex cavitation arising in a centrifugal pump," *Proc. Third I.Mech.E. Int. Conf. on Cavitation*, 1992, pp. 103-110.
- Sturtevant, B. and Kulkarny, V.J., "The focusing of weak shock waves," *J. Fluid Mech.*, 1996, Vol. 73, pp. 651-680.
- Ukon, Y., "Cavitation characteristics of a finite swept wing and cavitation noise reduction due to air injection," *Proc. of the Int. Symp. on Propeller and Cavitation*, 1986, pp. 383-390.
- van der Meulen, J.H.J. and van Renesse, R.L., "The collapse of bubbles in a flow near a boundary," *Proc. 17th ONR Symp. on Naval Hydrodynamics, The Hague*, 1989, pp. 195-217.
- van Wijngaarden, L., "On the collective collapse of a large number of gas bubbles in water," *Proc. 11th Int. Conf. Appl. Mech.*, Springer-Verlag, Berlin, 1964, pp. 854-861.
- Vogel, A., Lauterborn, W. and Timm, R., "Optical and acoustic investigations of dynamics of the laser-produced cavitation bubbles near a solid boundary layer," *J. Fluid Mech.*, 1989, Vol. 206, pp. 299-338.
- Wade, R.B. and Acosta, A.J., "Experimental observations on the flow past a plano-convex hydrofoil," *ASME J. Basic Eng.*, 1966, Vol. 88, pp. 273-283.
- Wang, Y.-C. and Brennen, C.E., "Shock wave development in the collapse of a cloud of bubbles," *ASME Cavitation and Multiphase Flow Forum*, 1994, FED-Vol. 194, pp. 15-20.
- Wang, Y.-C. and Brennen, C.E., "The noise generated by the collapse of a cloud of cavitation bubbles," *ASME/JSME Symp. on Cavitation and Gas-Liquid Flow in Fluid Machinery and Devices*, 1995, FED-Vol. 226, pp. 17-29.
- Wang, Y.-C. and Brennen, C.E., "Shock wave and noise in the collapse of a cloud of cavitation bubbles," *20th Int. Symp. on Shock Waves, Pasadena*, 1995, pp. 1213-1218.
- Wang, Y.-C. and Brennen, C.E., "Shock waves in cloud cavitation," 1997, submitted for publication.